Biochemical Pharmacology 77 (2009) 1684–1693

Contents lists available at ScienceDirect

Biochemical Pharmacology

journal homepage: www.elsevier.com/locate/biochempharm

AMP-activated protein kinase-dependent and -independent mechanisms underlying in vitro antiglioma action of compound C

Ljubica Vucicevic [a,b], Maja Misirkic [a,b], Kristina Janjetovic [a,b], Ljubica Harhaji-Trajkovic [b], Marko Prica [a], Darko Stevanovic [c], Esma Isenovic [d], Emina Sudar [d], Mirjana Sumarac-Dumanovic [e], Dragan Micic [e], Vladimir Trajkovic [a,*]

[a] Institute of Microbiology and Immunology, School of Medicine, University of Belgrade, Dr. Subotica 1, 11000 Belgrade, Serbia
[b] Institute for Biological Research "Sinisa Stankovic", Belgrade, Serbia
[c] Institute of Physiology, School of Medicine, University of Belgrade, Belgrade, Serbia
[d] Laboratory for Molecular Genetics and Radiobiology, Vinca Institute of Nuclear Sciences, Belgrade, Serbia
[e] Institute of Endocrinology, Diabetes and Diseases of Metabolism, University Clinical Centre, Belgrade, Serbia

ARTICLE INFO

Article history:
Received 9 December 2008
Accepted 2 March 2009

Keywords:
Glioma
AMPK
Compound C
Apoptosis
Oxidative stress

ABSTRACT

We investigated the effect of compound C, a well-known inhibitor of the intracellular energy sensor AMP-activated protein kinase (AMPK), on proliferation and viability of human U251 and rat C6 glioma cell lines. Compound C caused G_2/M cell cycle block, accompanied by apoptotic glioma cell death characterized by caspase activation, phosphatidylserine exposure and DNA fragmentation. The mechanisms underlying the pro-apoptotic action of compound C involved induction of oxidative stress and downregulation of antiapoptotic molecule Bcl-2, while no alteration of pro-apoptotic Bax was observed. Compound C diminished AMPK phosphorylation and enzymatic activity, resulting in reduced phosphorylation of its target acetyl CoA carboxylase. AMPK activators metformin and AICAR partly prevented the cell cycle block, oxidative stress and apoptosis induced by compound C. The small interfering RNA (siRNA) targeting of human AMPK mimicked compound C-induced G_2/M cell cycle arrest, but failed to induce oxidative stress and apoptosis in U251 glioma cells. In conclusion, our data indicate that AMPK inhibition is required, but not sufficient for compound C-mediated apoptotic death of glioma cells.

1. Introduction

Adenosine monophosphate-activated protein kinase (AMPK) is a principal intracellular energy sensor which activates energy-producing pathways and inactivates energy-requiring pathways when the cellular AMP/ATP ratio is increased [1]. Stimuli such as hypoxia, nutrient deprivation and some hormones/cytokines, activate AMPK through phosphorylation of Thr-172 within catalytic α subunit of the heterotrimeric AMPK enzymatic complex [1]. In its active state, AMPK switches on catabolic pathways that generate ATP, such as fatty acid oxidation, glucose uptake and glycolysis, while switches off ATP-consuming anabolic pathways such as fatty acid and cholesterol biosynthesis [1]. AMPK mediates these effects through direct phosphorylation of target proteins, as well as by controlling gene expression. The role of AMPK in cancer is still not fully understood and the data obtained so far appear to be conflicting. A considerable body of evidence indicates that excessive AMPK activation inhibits the growth and/or survival of various cancer cell lines [2–8]. On the other hand, a certain level of AMPK activity might be required for optimal cell proliferation and survival in stress conditions. Accordingly, tumor xenografts prepared from Ras-transformed mouse embryo fibroblasts lacking AMPK lost their ability to grow in hypoxic environment [9], and PC12 pheochromocytoma cells transfected with dominant-negative AMPK underwent apoptosis upon glucose deprivation [10]. Moreover, compound C, a cell-permeable pyrrazolopyrimidine derivative that acts as a potent, selective ATP-competitive inhibitor of AMPK [11], was found to induce apoptosis in myeloma cell lines in the absence of any stress [12]. Therefore, pharmacological inhibition of AMPK activity might be potentially useful in therapy of certain types of cancer.

Malignant gliomas are among the most lethal cancers, which are notoriously difficult to treat due to resistance to apoptosis induction with traditional chemotherapeutics and radiation [13]. In order to develop new therapies, there is a great research effort in understanding the molecular mechanisms underlying glioma

* Corresponding author. Tel.: +381 11 3643 233; fax: +381 11 3643 235.
E-mail address: vtrajkovic@eunet.rs (V. Trajkovic).

0006-2952/$ – see front matter © 2009 Elsevier Inc. All rights reserved.
doi:10.1016/j.bcp.2009.03.005

pathogenesis and progression. Oncogenic modification in gliomas is frequently associated with upregulation of cell proliferation/survival-regulating signaling pathways, such as those controlled by PI-3 kinase/Akt/mTOR and protein kinase C, leading to their constitutive activation and uncontrolled growth and invasion [14]. AMPK activation has recently been found to induce proliferation block and apoptosis in glioma cells by suppressing the mTOR pathway [3]. Glioma cell death induced by pharmacological activation of AMPK was mediated by reactive oxygen species (ROS) [7], consistent with the role of oxidative stress in activating pro-apoptotic and blocking survival signals in glioma cells [15,16]. However, the effect of AMPK inhibition on glioma cell proliferation and viability has not been assessed thus far.

The present study for the first time demonstrates that compound C, a well-known AMPK antagonist, inhibits proliferation and induces oxidative stress-mediated apoptotic cell death in glioma cell lines. Interestingly, while proliferation block was mediated solely by AMPK inhibition, both AMPK-dependent and -independent mechanisms were apparently involved in the induction of oxidative stress and apoptosis in compound C-treated glioma cells.

2. Materials and methods

2.1. Cell culture

The rat glioma cell line C6 and the human glioma cell line U251 were kindly donated by Dr. Pedro Tranque (Universidad de Castilla-La Mancha, Albacete, Spain), while the mouse B16 melanoma cell line was obtained from the European Collection of Animal Cell Cultures (Salisbury, UK). The primary astrocytes were isolated from brains of newborn Albino Oxford rats as previously described [17], in accordance with the Declaration of Helsinki. The tumor cell lines and primary astrocytes were maintained at 37 °C in a humidified atmosphere with 5% CO_2, in a HEPES (20 mM)-buffered RPMI 1640 cell culture medium (Sigma–Aldrich, St. Louis, MO) supplemented with 5% fetal calf serum, 2 mM L-glutamine, 10 mM sodium pyruvate and penicillin/streptomycin (all from Sigma–Aldrich). The cells were prepared for experiments using the conventional trypsinization procedure with trypsin/EDTA (Sigma–Aldrich, St. Louis, MO) and incubated in 96-well flat-bottom plates (1×10^4 cells/well) for the cell viability assessment and cell-based ELISA, 24-well plates (5×10^4 cells/well) for the flow cytometric analysis, or 90 mm Petri dishes (2×10^6 cells) for the Western blotting. Cells were rested for 24 h and then treated with compound C (6-[4-(2-piperidin-1-ylethoxy)phenyl]-3-pyridin-4-ylpyrazolo[1,5-a]pyrimidine; Sigma–Aldrich, St. Louis, MO), in the absence or presence of the antioxidants N-acetylcysteine and butylated hydroxyanisole (both from Sigma–Aldrich), or AMPK activators metformin (Hemofarm, Vrsac, Serbia) and 5-aminoimidazole-4-carboxamide-1-beta-D-ribofuranoside (AICAR; Sigma–Aldrich), as described in Section 3 and figure legends. Since compound C (50 mM) was initially dissolved in DMSO, the control cell cultures contained the appropriate amount of DMSO.

2.2. Determination of cell number and mitochondrial dehydrogenase activity

The cell number and mitochondrial dehydrogenase activity, as indicators of cell viability, were determined as previously described, using crystal violet staining and MTT [3-(4,5-dimethylthiazol-2-yl)-2,5-diphenyltetrazolium bromide] assay, respectively [18]. The crystal violet or MTT (both from Sigma–Aldrich, St. Louis, MO) absorbance was measured in an automated microplate reader at 570 nm. The results were presented as % of the control value obtained in untreated cells.

2.3. Cell cycle and apoptosis analysis

The cell cycle was analyzed by measuring the amount of propidium iodide (PI)-labeled DNA in fixed cells, as previously described [19]. Apoptotic cell death was analyzed by double staining with annexin V-FITC and PI, in which annexin V binds to early apoptotic cells with exposed phosphatidylserine, while PI labels the late apoptotic/necrotic cells with a membrane damage. Staining was performed according to the instructions by the manufacturer (BD Pharmingen, San Diego, CA). A green/red (FL1/FL2) fluorescence of annexin/PI- and PI-stained cells was analyzed with FACSCalibur flow cytometer (BD, Heidelberg, Germany), using FL2-W/FL1-A dot plot to exclude cell aggregates during cell cycle analysis. The numbers of viable (annexin$^-$/PI$^-$), early apoptotic (annexin$^+$/PI$^-$) and late apoptotic/necrotic (annexin$^+$/PI$^+$) cells, as well as the proportion of cells in different cell cycle phases, including sub-G compartment with hypodiploid, apoptotic cells, were determined with a Cell Quest Pro software (BD).

2.4. Caspase activation

Activation of caspases was measured by flow cytometry after labeling the cells with a cell-permeable, FITC-conjugated pan-caspase inhibitor (ApoStat; R&D Systems, Minneapolis, MN) or caspase-3- and caspase-8-selective reagents (Vybrant® Caspase Assay kit; Invitrogen, Paisley, UK) according to the manufacturer's instructions. The increase in green fluorescence (FL1) as a measure of caspase activity within individual cells of the treated population was determined using FACSCalibur flow cytometer. The results are expressed as % of cells containing active caspases. The caspase-3-specific inhibitor Z-DEVD-fmk was purchased from R&D Systems (Minneapolis, MN).

2.5. ROS determination

Intracellular production of ROS was determined by measuring the intensity of green fluorescence emitted by non-selective redox-sensitive dye dihydrorhodamine 123 (DHR; Invitrogen, Paisley, UK). The production of superoxide was measured using superoxide-selective fluorochrome dihydroethidium (DHE; Invitrogen, Paisley, UK). DHR (5 μM) was added to cell cultures at the beginning of treatment, while DHE (20 μM) was incubated with the cells for the last 30 min of the treatment. At the end of incubation, cells were detached by trypsinization and washed with PBS. The mean intensity of green (FL1, DHR) or red (FL2, DHE) fluorescence, corresponding to total ROS levels of superoxide amount, respectively, was determined using a FACSCalibur flow cytometer.

2.6. Western blot detection of activated AMPK

The cells were lysed in a lysis buffer (30 mM Tris–HCl pH 8.0, 150 mM NaCl, 1% NP-40, 1 mM phenylmethylsulfonylfluoride and protease inhibitor cocktail; all from Sigma–Aldrich, St. Louis, MO) on ice for 30 min, centrifuged at 18,000 × *g* for 15 min at 4 °C, and the cell lysates were collected. Equal amounts of protein from each sample was separated by SDS-PAGE and transferred to nitrocellulose membranes (Bio-Rad, Marnes-la-Coquette, France). Following incubation with anti-phospho-AMPK, anti-AMPK (Santa Cruz Biotechnology, Santa Cruz, CA) or anti-β-actin antibodies (Abcam, Cambridge MA) as primary antibodies and peroxidase-conjugated goat anti-rabbit IgG (Jackson IP Laboratories, West Grove, PA) as a secondary antibody, specific bands corresponding to phospho-AMPK, total AMPK and β-actin were visualized using enhanced chemiluminescence reagents for Western blot analysis (Amersham

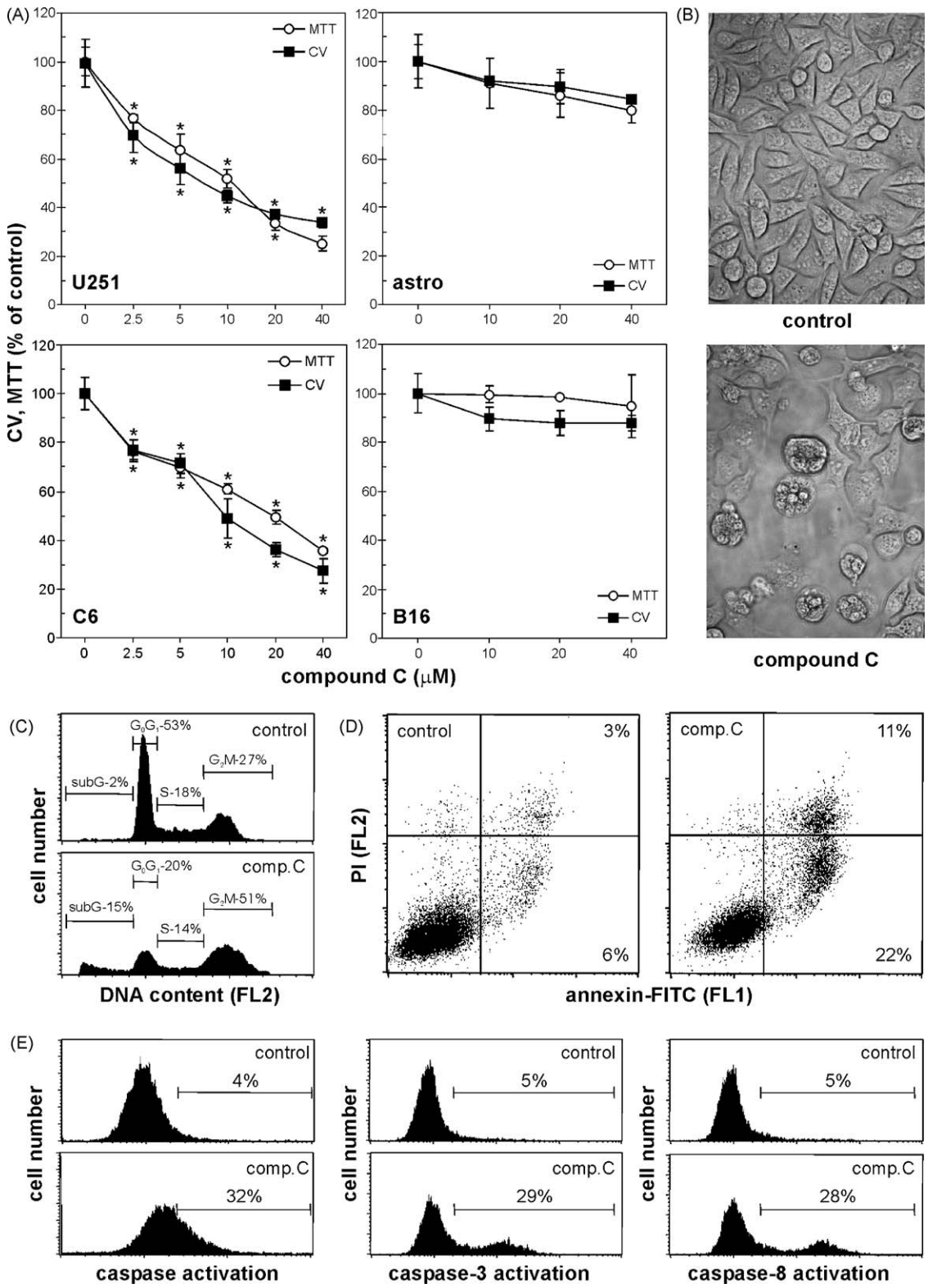

Fig. 1. Compound C induces cell cycle arrest and apoptosis in glioma cells. (A) U251 glioma cells, C6 glioma cells, rat primary astrocytes and B16 melanoma cells were incubated with different concentrations of compound C, and the cell viability was determined by crystal violet (CV) or MTT assay after 48 h. The data from representative of three experiments are mean + SD values of triplicate observations ($^{*}p < 0.05$). (B–E) U251 cells were incubated with compound C (20 μM) for 24 h. Cell morphology was examined by inverted microscopy (B). Alternatively, cells were stained with PI (C), annexin V-FITC/PI (D) or ApoStat (E), and the cell cycle (C), proportion of apoptotic (annexin^{+}) cells (D) or caspase activation (E) was examined by flow cytometry. The representative dot plots and histograms from at least three experiments are presented.

Pharmacia Biotech, Piscataway, NJ). The signal intensity was determined by densitometry and the results were presented as phospho-AMPK/total AMPK signal ratio, which was arbitrarily set to 1 in control.

2.7. ELISA for Bax, Bcl-2 and phospho-acetyl-CoA carboxylase (ACC)

The Bax and Bcl-2 levels in cell lysates were measured using ELISA kit (R&D Systems, Minneapolis, MN) according to manu-

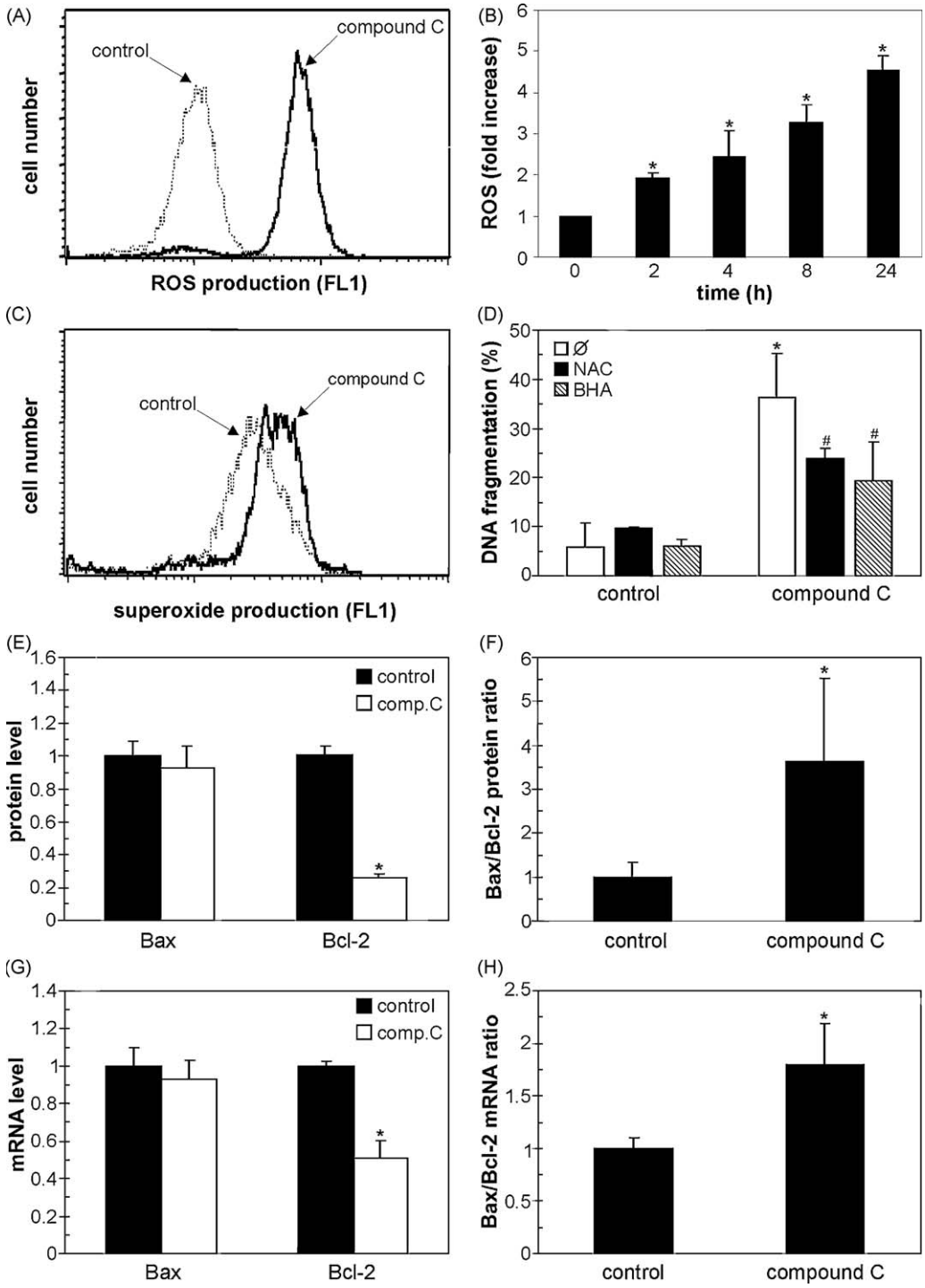

Fig. 2. Compound C induces ROS-dependent DNA fragmentation and Bax/Bcl-2 increase in glioma cells. (A–C) U251 cells were incubated with compound C (20 μM) for 24 h (A and C) or the indicated time periods (B). Flow cytometry was used to determine intracellular levels of total ROS in DHR-stained cells (A and B) or superoxide in DHE-stained cells (C). (D) U251 cells were incubated with compound C (20 μM) in the absence or presence of antioxidants N-acetylcysteine (NAC; 2 mM) or butylated hydroxyanisole (BHA; 50 μM). DNA fragmentation was determined by flow cytometry (PI staining) after 24 h. (E–H) The levels of Bax and Bcl-2 proteins (E) or mRNA (G) in compound C (20 μM)-treated U251 cells were measured by ELISA (18 h) or real-time RT-PCR (8 h), and the Bax/Bcl-2 protein (F) or mRNA (H) ratio was calculated. The representative flow cytometry histograms are presented in (A and C), the data in (B and D) are mean + SD values from three independent experiments, while the data in (E–H) are mean + SD values of triplicate observations from a representative of three experiments ($^{*}p < 0.05$ and $^{\#}p < 0.05$ refer to untreated and compound C-treated cells, respectively).

facturer's instructions. The phosphorylation of ACC was determined by cell-based ELISA [20], using anti-phospho-ACC (Abcam, Cambridge, MA) as a primary antibody, while peroxidase-conjugated goat anti-rabbit IgG (USB Corporation, Cleveland, OH) was used as a detecting antibody. The absorbance at 450 nm was measured in an automated microplate reader after incubation with peroxidase substrate TMB (Sigma–Aldrich, St. Louis, MO) and blocking with 0.1 M HCl. The results were normalized according to protein content (Bax, Bcl-2) or cell number (phospho-ACC) and presented as relative to the control value, which was arbitrarily set to 1.

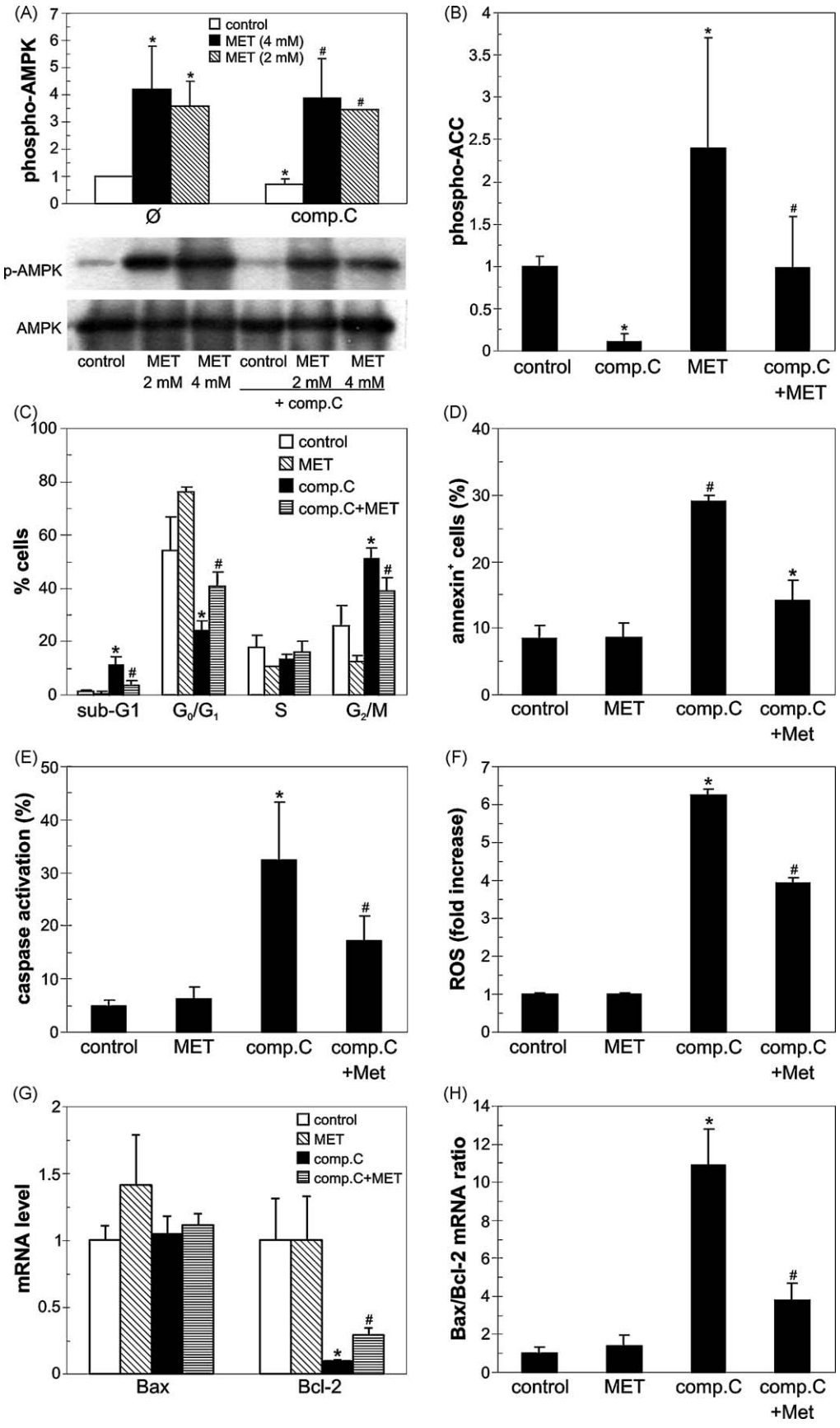

Fig. 3. Metformin prevents compound C-induced AMPK downregulation and apoptosis. (A and B) U251 cells were incubated with compound C (20 μM), in the absence or presence of the indicated concentrations (A) or 2 mM (B) of metformin. The intracellular concentrations of phospho-AMPK (A) and phospho-ACC (B) were determined after 8 h by Western blotting and cell-based ELISA, respectively. (C–H) C6 cells were treated with compound C (20 μM), in the absence or presence of metformin (2 mM). After 24 h, cells were stained with PI (C), annexin V-FITC/PI (D), ApoStat (E) or DHR (F), and cell cycle (C), phosphatidylserine externalization (D), caspase activation (E) or ROS production

2.8. Real-time RT-PCR for Bax and Bcl-2 mRNA

Total RNA was extracted using TRIZOL reagent (Invitrogen, Paisley, UK) according to the manufacturer's instructions. Approximately 1 μg of RNA was used in the reverse transcription reaction using M-MuLV RT with random hexamers (Fermentas, Vilnus, Lithuania) according to the manufacturer's instructions. Real-time RT-PCR was performed on ABI Prism 7500 thermocycler (Applied Biosystems, Foster City, CA) in a 96-well reaction plate (MicroAmp Optical, Foster City, CA). The reactions were prepared according to the standard protocol for one-step QuantiTect SYBR Green RT-PCR (Applied Biosystems, Cheshire, UK), using commercially available primers for Bax-α or Bcl-2 (R&D Systems, Minneapolis, MN), and human GAPDH (Applied Biosystems) or rat β-actin (Sigma–Aldrich, St. Louis, MO). Primers for β-actin were: 5′-CCCTGGCTCCTAGCACCAT-3′ (forward primer) 5′-GAGCCACCAATCCACACAGA-3′ (reverse primer), while GAPDH primers were 5′-CATCCATGACAACTTTGGTATCG-3′ (forward) and 5′-CCATCACGCCACAGTTTCC-3′ (reverse). Both GAPDH and β-actin primers were designed using Primer Express® software v2.0 (Applied Biosystems). Initial step of RT-PCR was 2 min at 50 °C, followed by a 10 min hold at 95 °C. Cycles ($n = 40$) consisted of a 15 s melt at 95 °C, followed by a 1 min annealing/extension at 60 °C. The final step was a 60 °C incubation for 1 min. All reactions were performed in triplicates. The cycle of threshold (Ct) analysis was set at 0.1 relative fluorescence units. Averaged Ct values of control triplicates (GAPDH or actin) were subtracted from Ct values of target genes to obtain ΔCt, and then relative gene expression was determined as $2^{-\Delta Ct}$. The results were presented relative to the control value, which was arbitrarily set to 1. The SD values for the Bax/Bcl-2 ratio were calculated as follows: $C \times \sqrt{(a^2/A^2 + b^2/B^2)}$, where C = Bax/Bcl-2 ratio, while a and b represent SD of Bax (A) and Bcl-2 values (B), respectively.

2.9. Transfection with small interfering RNA

Small interfering RNA (siRNA) targeting human AMPKα1/2, as well as scrambled control siRNA, were obtained from Santa Cruz Biotechnology (Santa Cruz, CA). Subconfluent U251 cells in 90 mM Petri dishes were transfected with AMPK and control siRNA according to the manufacturer's protocol. Briefly, cells were incubated in transfection medium (without FCS and antibiotics) containing siRNA (200 nm). After 8 h, an equal amount of 2× normal cell culture medium (with FCS and antibiotics) was added and cells were incubated for an additional 28 h. Cells were then replated in 96-well plates, 24-well plates or 90 mm Petri dishes as described in Section 2.1 and rested for 24 h. Subsequently, AMPK expression (Western blot), cell number (crystal violet), mitochondrial dehydrogenase activity (MTT), annexin binding, caspase activation and intracellular ROS levels (flow cytometry) were determined as outlined above and in figure legends.

2.10. Statistical analysis

The statistical significance of the differences was analyzed by t-test (two independent samples) or ANOVA (multiple comparisons). The value of $p < 0.05$ was considered significant.

3. Results

3.1. Compound C induces cell cycle arrest and apoptosis in glioma cells

C6 and U251 glioma cell lines were treated with different concentrations of compound C for 48 h, and the cell numbers and mitochondrial dehydrogenase activity were analyzed using crystal violet and MTT assay, respectively. Compound C decreased both the cell numbers and mitochondrial dehydrogenase activity in a dose-dependent manner (Fig. 1A). The observed effect was fairly specific for glioma cells, since compound C did not significantly affect the viability of rat primary astrocytes and mouse B16 melanoma cells (Fig. 1A). Microscopic examination revealed a considerable change in the morphology of compound C-treated U251 glioma cells. The cells lost their processes, became round and detached from the cell culture plastic, which is consistent with the induction of cell death (Fig. 1B). The exposure to compound C induced a cell cycle arrest in G_2/M phase, associated with an increase in the number of apoptotic, hypodiploid cells with fragmented DNA (sub-G_0/G_1), as demonstrated by flow cytometric analysis of PI-stained DNA in U251 glioma cells (Fig. 1C). The induction of apoptosis in compound C-exposed U251 cells was confirmed by annexin/PI-staining, which showed a significant increase in the proportion of early apoptotic (annexin$^+$PI$^-$) and late apoptotic/necrotic (annexin$^+$PI$^+$) cells (Fig. 1D). Compound C-mediated apoptotic death of U251 cells was associated with the activation of caspases, including caspase-3 and caspase-8, the key apoptosis-inducing members of the caspase enzyme family (Fig. 1E). The caspase-3-selective inhibitor markedly reduced compound C-triggered caspase-3 activation (from 34.5 ± 7.9 to 15.5 ± 6.6%; $n = 2$) and accumulation of annexin$^+$ cells (from 34.9 ± 6.1 to 18.6 ± 2.1; $n = 2$), thus confirming that U251 glioma cell death was caspase-mediated. Results similar to those presented in Fig. 1B–E were obtained with C6 cells (data not shown).

3.2. Compound C increases ROS production and Bax/Bcl-2 ratio in glioma cells

Since oxidative stress is a potent inducer of apoptosis, we next investigated if compound C could cause a production of ROS in glioma cells. Using a redox-sensitive fluorochrome DHR, we have observed a time-dependent increase of ROS generation in U251 cells, starting 2 h after compound C addition (Fig. 2A and B). At least part of compound C-triggered ROS production could be attributed to superoxide, as demonstrated by flow cytometric analysis of U251 cells stained with superoxide-selective fluorescent dye DHE (Fig. 2C). Accordingly, compound C-induced apoptosis, measured as DNA fragmentation, was efficiently diminished by the antioxidant agents N-acetylcysteine and butylated hydroxyanisole (Fig. 2D). We next assessed the influence of compound C on intracellular levels of important apoptosis-regulating proteins Bax and Bcl-2. The ELISA performed on cell lysates revealed a dramatic reduction of Bcl-2 concentration in U251 cells after treatment with compound C, while no effect on Bax protein levels was observed (Fig. 2E). As a result, the Bax/Bcl-2 ratio was markedly increased in compound C-exposed cells (Fig. 2F). Consistent with the ELISA results, RT-PCR demonstrated a significant reduction of intracellular levels of Bcl-2, but not Bax mRNA (Fig. 2G), as well as a consequent increase in Bax/Bcl-2 mRNA ratio in compound C-treated U251 cells (Fig. 2H). Results similar to those presented in Fig. 2A–H were obtained with C6 glioma cells (see Fig. 3).

3.3. AMPK activators metformin and AICAR reduce compound C-triggered cell cycle block and apoptosis

We next assumed that the observed pro-apoptotic effect of compound C on glioma cells could be a consequence of the

(F) was examined by flow cytometry. Bax and Bcl-2 mRNA levels were assessed by real-time RT-PCR after 8 h (G) and Bax/Bcl-2 mRNA ratio was calculated (H). The data are mean + SD values from three (A, B, D–F) or four (C) separate experiments, or mean + SD of triplicates from one of two experiments with similar results (G and H) ($^*p < 0.05$ and $^\#p < 0.05$ refer to untreated and compound C-treated cells, respectively).

inhibition of AMPK activation and/or enzymatic activity. To test this hypothesis, a Western blot analysis of Thr-172 phosphorylation in the AMPK active site was performed in glioma cells treated with compound C alone or in combination with metformin, a well-known AMPK activator. Compound C reduced AMPK phosphorylation in C6 glioma cells by 30% (Fig. 3A), while metformin markedly augmented AMPK activation and completely prevented compound C-induced inhibition of AMPK activation (Fig. 3A). To assess the enzymatic activity of AMPK, we performed cell-based ELISA to detect phosphorylation of the AMPK substrate ACC. Compound C almost completely prevented ACC phosphorylation in C6 cells, while metformin alone increased ACC phosphorylation and completely neutralized the inhibitory action of compound C (Fig. 3B). To further explore the role of AMPK inhibition in compound C-mediated antiglioma action, we tested the ability of metformin to reduce various parameters of apoptotic cell demise

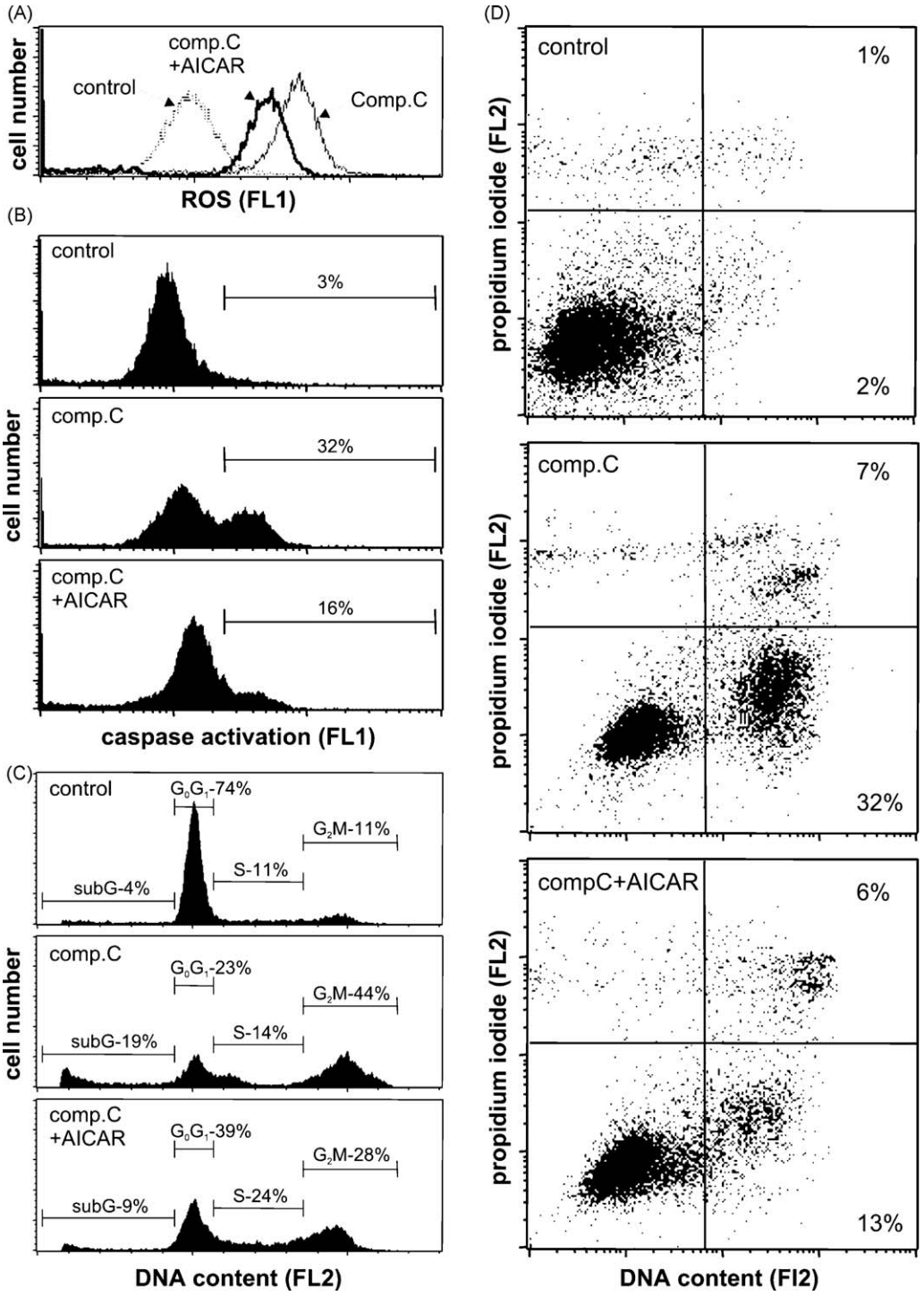

Fig. 4. AICAR prevents compound C-induced glioma cell apoptosis. (A–D) U251 cells were incubated with compound C (20 μM), in the absence or presence of AICAR (250 μM). After 24 h, cells were stained with DHR (A), ApoStat (B), PI (C) or annexin V-FITC/PI (D), and ROS production (A) caspase activation (B), cell cycle (C) and phosphatidylserine externalization (D) were examined by flow cytometry. The histograms and dot plots from one of two independent experiments with similar results are presented.

in compound C-treated glioma cell cultures. Although metformin itself caused a G_0/G_1 cell cycle arrest in C6 cells, it efficiently prevented compound C-induced cell cycle disturbances, i.e. G_2/M block and sub-G_0/G_1 accumulation (Fig. 3C). In addition, compound C-triggered phosphatidylserine externalization (Fig. 3D), caspase activation (Fig. 3E), ROS generation (Fig. 3F), and decrease in Bcl-2 mRNA levels and Bax/Bcl-2 ratio (Fig. 3G and H) were all efficiently counteracted by metformin. Similar effects of metformin on compound C-mediated apoptosis were also observed in U251 cells (not shown). Another AMPK activator, AICAR, was also able to reduce oxidative stress (Fig. 4A), caspase activation (Fig. 4B), G_2/M cell cycle block, DNA fragmentation (Fig. 4C), and phosphatidylserine externalization (Fig. 4D) in compound C-treated U251 cells.

3.4. AMPK inhibition is not sufficient for the induction of oxidative stress and apoptosis

The protective effect of metformin and AICAR in compound C-treated glioma cells indicated a possible involvement of AMPK inhibition in antiglioma action of compound C. To further investigate this possibility, we transfected U251 cells with siRNA against AMPK and measured the cell viability and various apoptotic parameters. The downregulation of AMPK in siRNA-transfected cells was confirmed by Western blotting (Fig. 5A). As a result of AMPK silencing, the phosphorylation of ACC was markedly suppressed for at least 48 h following seeding of AMPK siRNA-transfected cells (Fig. 5B). The crystal violet and MTT tests revealed that cell numbers and mitochondrial dehydrogenase

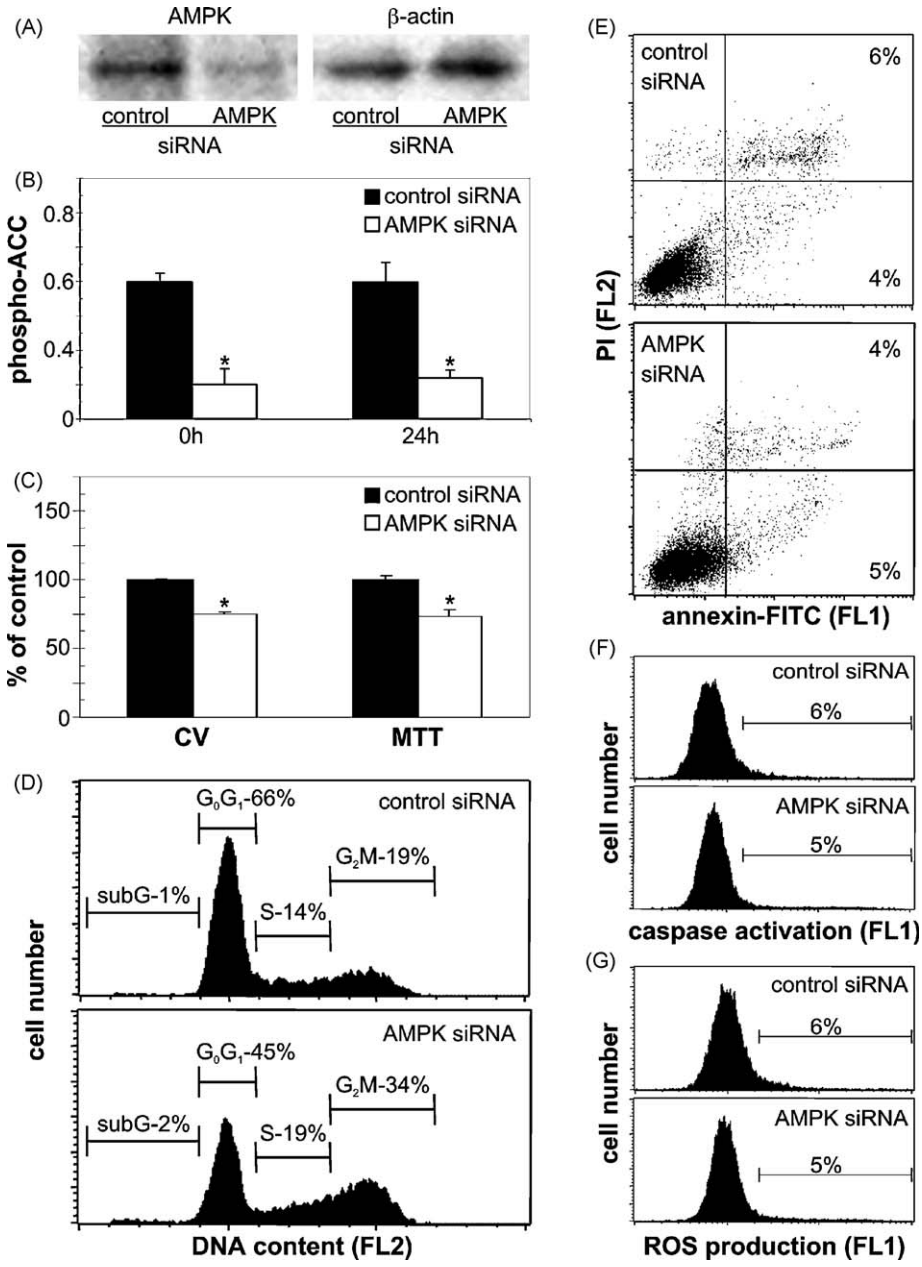

Fig. 5. The effects of AMPK silencing in U251 cells. (A–G) U251 cells were transfected with control or AMPK-targeting siRNA and replated as described in Section 2. The intracellular levels of AMPK were determined by Western blotting after 24 h (A), the cell-based ELISA for phospho-ACC was performed after 24 and 48 h (B), while crystal violet and MTT assay were performed 72 h after replating the transfected cells (C). Cell cycle distribution (PI staining; D), apoptosis (annexin V-FITC/PI staining; E), caspase activation (ApoStat staining; F) and total ROS production (DHR staining; G) were determined by flow cytometry 48 h after replating the transfected cells. The data in (A–G) are from one of two experiments with similar results. The data in (B and C) are mean + SD of triplicates ($^*p < 0.05$).

activity were reduced in AMPK siRNA-transfected U251 cells, in comparison to those transfected with control siRNA (Fig. 5C). Accordingly, AMPK siRNA-transfected cells displayed a cell cycle arrest in G_2/M phase (Fig. 5D). On the other hand, siRNA-mediated downregulation of AMPK activity in glioma cells failed to induce oxidative stress, caspase activation, phosphatidylserine exposure and DNA fragmentation in U251 cells (Fig. 5E–G). The oxidative stress and apoptotic events were measured 48 h after seeding the transfected cells, when AMPK enzymatic activity was still markedly suppressed (Fig. 5B), thus excluding the possibility that the absence of apoptosis was due to AMPK reactivation. Therefore, although able to induce G_2/M cell cycle arrest, AMPK inhibition alone was not sufficient for the induction of oxidative stress and apoptosis in glioma cells.

4. Discussion

The present study demonstrates that AMPK inhibitor compound C exerts a potent antiglioma activity in vitro, causing cell cycle arrest and caspase-dependent glioma cell apoptosis. The mechanisms underlying the antiglioma effect of compound C included induction of oxidative stress and Bcl-2 downregulation, followed by caspase activation and subsequent execution of apoptotic cell death characterized by phosphatidylserine exposure and DNA fragmentation. Interestingly, AMPK inhibition was required, but not sufficient for glioma cell apoptosis in our study, thus implicating the cooperation of the AMPK-dependent and -independent mechanisms in compound C-induced apoptotic death of glioma cells (Fig. 6).

Having in mind the energy-saving role of AMPK, it is conceivable that it may act to protect cells in a variety of stress conditions, including hypoxia or glucose deprivation [9,10]. The protective action of AMPK is not restricted to nutrient stress, as this enzyme seems to play an important role in protecting tumor cells from apoptosis induced by chemotherapeutic agents such as cisplatin [21]. Moreover, transfection with dominant-negative AMPK was sufficient to reduce proliferation of HeLa cervical carcinoma and PC12 pheochromocytoma cells in the absence of any stress [10]. In accordance with these findings, our data support the role of AMPK in maintaining optimal proliferation rate in cultures of U251 and C6 glioma cell lines. On the other hand, rat primary astrocytes and B16 melanoma cells were fairly resistant to pharmacological blockade of AMPK activity. Even though we presently have not pursued the mechanisms underlying this phenomenon, it is possible that compound C-resistant cell types have higher basal AMPK activity compared to glioma cells, or that the ability of AMPK to support cell proliferation is cell-type dependent. The latter might be due to differences in requirements for glycolysis in distinct cell types, which is consistent with the well-documented high glycolytic phenotype of glioma cells [22,23], and the fact that AMPK is one of the crucial glycolysis activators [24].

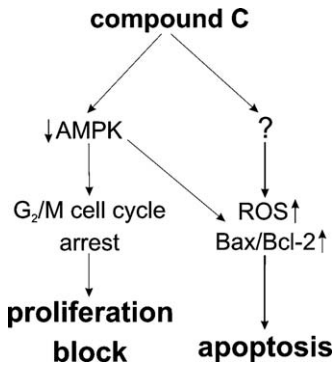

Fig. 6. Hypothetical mechanisms of compound C-mediated antiglioma action. Compound C-mediated inhibition of AMPK is sufficient for the cell cycle arrest, but requires cooperation with the unknown mechanism(s) to cause apoptosis in glioma cells.

In addition to inducing cell cycle arrest, compound C treatment caused apoptotic death of glioma cells. The main mechanism underlying the pro-apoptotic action of compound C was the induction of ROS generation, as revealed by the protective effect of antioxidant treatment. Besides directly contributing to cell injury by causing mitochondrial damage and oxidation of proteins, lipids and DNA [25], oxidative stress is also involved in transcriptional and post-transcriptional perturbation of the balance between apoptosis-regulating Bcl-2 family members Bax and Bcl-2 [26,27]. In our study, compound C-mediated increase in ROS production was accompanied by a decrease in both mRNA and protein Bcl-2 levels and no change in Bax expression, resulting in a shift of Bax/Bcl-2 ratio towards pro-apoptotic Bax. Similarly, compound C-induced apoptosis in multiple myeloma cells was accompanied by downregulation of Bcl-2 family members Bcl-xl and Mcl-1 [12]. As a consequence, Bax could not be efficiently sequestered by Bcl-2 and it is being inserted into mitochondrial membrane, leading to its disruption and release of caspase-activating small molecules such as cytochrome C and Smac/Diablo [28]. Such a scenario is consistent with our findings showing the activation of caspase-3, which belongs to the above described mitochondrial pathway of apoptosis. Nevertheless, the activation of the death-receptor pathway-associated caspase-8 in compound C-treated glioma cells is not surprising, having in mind that caspase-8 could also be activated via the caspase-3 and -6 mediated interchain proteolysis during mitochondria-dependent apoptosis [29].

The ability of AMPK activators metformin and AICAR to protect compound C-exposed glioma cells supports the involvement of AMPK inhibition in compound C-triggered glioma cell apoptosis. On the other hand, siRNA-mediated AMPK silencing reduced proliferation of glioma cells, but it completely failed to mimic the pro-apoptotic action of compound C. Similarly, the transfection with dominant-negative AMPK caused proliferation block, but not apoptosis in HeLa cervical carcinoma and PC12 neuroblastoma cells [10], which, in conjunction with our data, confirms that AMPK inactivation alone is not sufficient to initiate apoptotic cascade. Although metformin has been reported to alter mitochondrial membrane potential in an AMPK-independent fashion [30,31], it does not seem very likely that both metformin and AICAR protected compound C-treated glioma cells independently of AMPK. Such a notion is further supported by our findings that oligomycin, another AMPK activator, shared the ability of metformin and AICAR to protect glioma cell from compound C-induced apoptosis (Vucicevic et al., unpublished observation). Therefore, a more conceivable explanation for the observed discrepancy is that the AMPK inhibition synergized with some other intracellular event(s) in the induction of apoptosis, thus being required, but not sufficient for compound C-mediated glioma cell death (Fig. 6).

In conclusion, the present study indicates that glioma cell treatment with compound C causes the AMPK inhibition-dependent cell cycle block, accompanied by oxidative stress-mediated apoptotic cell death exerted through cooperation of both AMPK-dependent and -independent mechanisms. These findings imply that the experiments in which compound C is used to selectively inhibit AMPK should be interpreted with caution, particularly if cytototoxic/cytoprotective effects are studied. Nevertheless, the putative AMPK-dependent component of compound C proaptotic action is consistent with the role of AMPK in maintaining glioma cell growth and viability, thus supporting potential therapeutic usefulness of pharmacologically targeting this key intracellular energy sensor.

Acknowledgements

This work was supported by the Ministry of Science of the Republic of Serbia (Grants Nos. 145073, 145067 and 143030). The authors thank Verica Paunovic for the assistance in manuscript preparation.

References

[1] Hardie DG, Hawley SA, Scott JW. AMP-activated protein kinase—development of the energy sensor concept. J Physiol 2006;574:7–15.
[2] Campàs C, Lopez JM, Santidrián AF, Barragán M, Bellosillo B, Colomer D, et al. Acadesine activates AMPK and induces apoptosis in B-cell chronic lymphocytic leukemia cells but not in T lymphocytes. Blood 2003;101:3674–80.
[3] Kefas BA, Cai Y, Kerckhofs K, Ling Z, Martens G, Heimberg H, et al. Metformin-induced stimulation of AMP-activated protein kinase in beta-cells impairs their glucose responsiveness and can lead to apoptosis. Biochem Pharmacol 2004;68:409–16.
[4] Saitoh M, Nagai K, Nakagawa K, Yamamura T, Yamamoto S, Nishizaki T. Adenosine induces apoptosis in the human gastric cancer cells via an intrinsic pathway relevant to activation of AMP-activated protein kinase. Biochem Pharmacol 2004;67:2005–11.
[5] Rattan R, Giri S, Singh AK, Singh I. 5-Aminoimidazole-4-carboxamide-1-beta-D-ribofuranoside inhibits cancer cell proliferation in vitro and in vivo via AMP-activated protein kinase. J Biol Chem 2005;280:39582–93.
[6] Zhou W, Han WF, Landree LE, Thupari JN, Pinn ML, Bililign T, et al. Fatty acid synthase inhibition activates AMP-activated protein kinase in SKOV3 human ovarian cancer cells. Cancer Res 2007;67:2964–71.
[7] Isakovic A, Harhaji L, Stevanovic D, Markovic Z, Sumarac-Dumanovic M, Starcevic V, et al. Dual antiglioma action of metformin: cell cycle arrest and mitochondria-dependent apoptosis. Cell Mol Life Sci 2007;64:1290–302.
[8] Okoshi R, Ozaki T, Yamamoto H, Ando K, Koida N, Ono S, et al. Activation of AMP-activated protein kinase induces p53-dependent apoptotic cell death in response to energetic stress. J Biol Chem 2008;283:3979–87.
[9] Laderoute KR, Amin K, Calaoagan JM, Knapp M, Le T, Orduna J, et al. 5'-AMP-activated protein kinase (AMPK) is induced by low-oxygen and glucose deprivation conditions found in solid-tumor microenvironments. Mol Cell Biol 2006;26:5336–47.
[10] Shaw MM, Gurr WK, McCrimmon RJ, Schorderet DF, Sherwin RS. 5'AMP-activated protein kinase alpha deficiency enhances stress-induced apoptosis in BHK and PC12 cells. J Cell Mol Med 2007;11:286–98.
[11] Zhou G, Myers R, Li Y, Chen Y, Shen X, Fenyk-Melody J, et al. Role of AMP-activated protein kinase in mechanism of metformin action. J Clin Invest 2001;108:1167–74.
[12] Baumann P, Mandl-Weber S, Emmerich B, Straka C, Schmidmaier R. Inhibition of adenosine monophosphate-activated protein kinase induces apoptosis in multiple myeloma cells. Anticancer Drugs 2007;18:405–10.
[13] Giese A, Bjerkvig R, Berens ME, Westphal M. Cost of migration: invasion of malignant gliomas and implications for treatment. J Clin Oncol 2003;21:1624–36.
[14] Sathornsumetee S, Reardon DA, Desjardins A, Quinn JA, Vredenburgh JJ, Rich JN. Molecularly targeted therapy for malignant glioma. Cancer 2007;110:13–24.
[15] Sonoda Y, Watanabe S, Matsumoto Y, Aizu-Yokota E, Kasahara T. FAK is the upstream signal protein of the phosphatidylinositol 3-kinase-Akt survival pathway in hydrogen peroxide-induced apoptosis of a human glioblastoma cell line. J Biol Chem 1999;274:10566–70.
[16] Kitamura Y, Ota T, Matsuoka Y, Tooyama I, Kimura H, Shimohama S, et al. Hydrogen peroxide-induced apoptosis mediated by p53 protein in glial cells. Glia 1999;25:154–64.
[17] McCarthy KD, de Vellis J. Preparation of separate astroglial and oligodendroglial cell cultures from rat cerebral tissue. J Cell Biol 1980;85:890–2.
[18] Mijatovic S, Maksimovic-Ivanic D, Radovic J, Miljkovic D, Kaludjerovic GN, Sabo TJ, et al. Aloe emodin decreases the ERK-dependent anticancer activity of cisplatin. Cell Mol Life Sci 2005;62:1275–82.
[19] Kaludjerovic GN, Miljkovic D, Momcilovic M, Djinovic VM, Mostarica Stojkovic M, Sabo TJ, et al. Novel platinum(IV) complexes induce rapid tumor cell death in vitro. Int J Cancer 2005;116:479–86.
[20] Versteeg HH, Nijhuis E, van den Brink GR, Evertzen M, Pynaert GN, van Deventer SJ, et al. A new phosphospecific cell-based ELISA for p42/p44 mitogen-activated protein kinase (MAPK), p38 MAPK, protein kinase B and cAMP-response-element-binding protein. Biochem J 2000;350:717–22.
[21] Kim HS, Hwang JT, Yun H, Chi SG, Lee SJ, Kang I, et al. Inhibition of AMP-activated protein kinase sensitizes cancer cells to cisplatin-induced apoptosis via hyper-induction of p53. J Biol Chem 2008;283:3731–42.
[22] Jelluma N, Yang X, Stokoe D, Evan GI, Dansen TB, Haas-Kogan DA. Glucose withdrawal induces oxidative stress followed by apoptosis in glioblastoma cells but not in normal human astrocytes. Mol Cancer Res 2006;4:319–30.
[23] Ziegler A, von Kienlin M, Décorps M, Rémy C. High glycolytic activity in rat glioma demonstrated in vivo by correlation peak ^{1}H magnetic resonance imaging. Cancer Res 2001;61:5595–600.
[24] Marsin AS, Bouzin C, Bertrand L, Hue L. The stimulation of glycolysis by hypoxia in activated monocytes is mediated by AMP-activated protein kinase and inducible 6-phosphofructo-2-kinase. J Biol Chem 2002;277:30778–83.
[25] Moreira PI, Smith MA, Zhu X, Nunomura A, Castellani RJ, Perry G. Oxidative stress and neurodegeneration. Ann NY Acad Sci 2005;1043:545–52.
[26] Li D, Ueta E, Kimura T, Yamamoto T, Osaki T. Reactive oxygen species (ROS) control the expression of Bcl-2 family proteins by regulating their phosphorylation and ubiquitination. Cancer Sci 2004;95:644–50.
[27] Gao X, Xu X, Pang J, Zhang C, Ding JM, Peng X, et al. NMDA receptor activation induces mitochondrial dysfunction, oxidative stress and apoptosis in cultured neonatal rat cardiomyocytes. Physiol Res 2007;56:559–69.
[28] Antonsson B. Bax and other pro-apoptotic Bcl-2 family "killer-proteins" and their victim the mitochondrion. Cell Tissue Res 2001;306:347–61.
[29] Sohn D, Schulze-Osthoff K, Jänicke RU. Caspase-8 can be activated by interchain proteolysis without receptor-triggered dimerization during drug-induced apoptosis. J Biol Chem 2005;280:5267–73.
[30] Carvalho C, Correia S, Santos MS, Seiça R, Oliveira CR, Moreira PI. Metformin promotes isolated rat liver mitochondria impairment. Mol Cell Biochem 2008;308:75–83.
[31] Hinke SA, Martens GA, Cai Y, Finsi J, Heimberg H, Pipeleers D, et al. Methyl succinate antagonises biguanide-induced AMPK-activation and death of pancreatic beta-cells through restoration of mitochondrial electron transfer. Br J Pharmacol 2007;150:1031–43.